ISBN: 978-3-95450-184-7 doi:10.18429/JACoW-IPAC2018-TUPMK005

CSR SHIELDING EFFECT IN DOGLEG AND EEX BEAMLINES

Gwanghui Ha, Pohang Accelerator Laboratory, Pohang, Gyeongbuk 790-784, KOREA
John Gorham Power, Manoel Conde, and Eric Wisniewski, Argonne National Laboratory, Argonne, IL 60439, USA

Abstract

CSR shielding is a well-known CSR suppression scheme which works by cutting off the low frequency CSR radiation. Although the shielding scheme is well known, its effects on the beam has been rarely studied. We investigate the CSR effect on the beam emittance when passing through a dogleg and a double dogleg type EEX beamline. An experimental study is planned at the Argonne Wakefield Accelerator facility where we can generate a 0.1-100 nC electron beam with an energy of 50 MeV and have a double dogleg EEX beamline. Tunable shielding plates are installed at the dipole magnet chambers of the EEX beamline to vary the shielding condition. Transverse and longitudinal phase space measurement systems are prepared to characterize the beam-CSR interaction, and bolometer and interferometry are prepared to characterize CSR. We present simulation results and preliminary experimental results.

INTRODUCTION

CSR is one of the key beam dynamics issue in modern accelerator design due to its significant impact on the beam quality. There have been many efforts to mitigate the CSR effect [1-5], and the CSR shielding is one of the effective methods considered for a long time [1]. The shielding suppresses the CSR power whose frequency is lower than the critical frequency corresponding to the shielding gap [6,7]. Since this method directly suppresses CSR, it can be used with other mitigation methods so that the CSR effect can be effectively suppressed.

This promising suppression method has been studied theoretically and experimentally [6-8], but these work was limited to an analysis for a single dipole magnet. Since the CSR effect on the beam is the result of coupled dynamics between CSR, incident beam characteristic, and beamline optics, the beam quality improvement for the single dipole would not guarantee the improvement for the full beamline. We want to investigate the impact of the shielding on the practical beamlines (dogleg and EEX) to understand the shielding effect and confirm if it helps to improve the beam quality.

The experiment is planned to use a single EEX beamline installed at Argonne Wakefield Accelerator facility (see Fig. 1) [9]. We can investigate the shielding effect on the two doglegs and EEX beamline by turning off and on the deflecting cavity. This experiment has three goals as below.

- Benchmark of CSR and CSR shielding algorithm
- What shielding do on the beam in real beamline
- Confirm if shielding improve the beam quality

Various incident beam conditions will be prepared using injector setting, and the phase spaces of the beam after the beamline will be measured to analyse the CSR shielding effect.

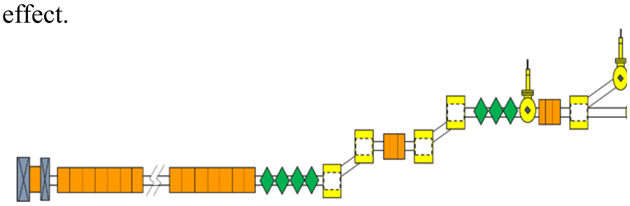

Figure 1: Schematic of emittance exchange beamline at Argonne Wakefield Accelerator facility.

TUNABLE GAP CHAMBER

The shielding suppresses the radiations whose frequency is lower than the critical frequency. This critical frequency is determined by the size of the chamber [6,7]. To investigate the shielding effect, we prepared the vacuum chamber for dipole magnets with tunable gap (see Fig. 2). Note, since it is hard to use a small beam pipe for all beamline due to the transverse optics issue with high charge beam (1-10 nC), we only use a tunable chamber for the dipole magnets.

Figure 2 is the picture of the tunable gap chamber. Three manual actuator hold top and bottom plates. Its maximum opening is 46 mm and we can set it to specific gap size with ~100 μm accuracy. Practically the minimum opening we can go is about 20 mm due to the beam transport without charge loss.

The beamline consists of two doglegs with rectangular magnet and the TDC in the middle. AWA drive beamline can generate various charge levels (0.1-100 nC) and the bunch lengths. There are four quadrupole magnets in front of the beamline to manipulate the transverse beam conditions. At the downstream of the beamline, quadrupole magnets, slit, dipole magnet and deflecting cavity are located so that we can measure both transverse and longitudinal phase spaces.

ISBN: 978-3-95450-184-7 doi:10.18429/JACoW-IPAC2018-TUPMK005

Figure 2: Picture of dipole chamber with tunable gap. There are movable plates at the top and bottom of the chamber. Each plate uses three manual actuator to locate it.

START-TO-END SIMULATION FOR SHIELDING STUDY

Here we show preliminary simulations using GPT [10] and CSR algorithm from Ref. [11]. Figure 3 shows the evolution of bunch length, energy spread, and mean energy for three difference cases along the double dogleg beamline (TDC off). The case 1 corresponding to (a-c) in Fig. 3 uses 10 nC beam with a relatively long bunch (>1 mm). The case 2 (d-f) uses 2 nC beam with a relatively short bunch (< 1 mm). The case 3 (g-i) uses 2 nC beam but the bunch length is relatively long (>1 mm). For each case, we compared 2 cm and 5 cm shielding gap results.

In terms of the shielding effect, Fig. 3 shows noticeable features. Firstly, smaller shielding gap suppresses the mean energy loss which means less CSR power. While the mean energy difference between 2 cm and 5 cm gap is clear for (c) and (i) (~100 keV and 50 keV respectively), it is only less than 10 keV for (f) which is short bunch case. Low frequency region is more dominant for the long bunch case than the short bunch case, so the cm-level gap is more effective to the long bunch case. These results follows the tendency expected from theory [6].

While the mean energy follows the theory, energy spread evolutions show different results. The shielding effect on the energy spread was controversial so far, but the BNL-ATF experiment in 2012 showed that the shielding suppresses the energy spread [8]. This is indeed true for the single dipole magnet. However, the simulation with a full beamline shows different tendency. 10 nC and long bunch case shows that the energy spread from 5 cm gap is larger than the spread from 2 cm gap at beginning but it becomes smaller at the end; see (b). 2 nC and short bunch case shows that the energy spread from 5 cm is lower at the beginning but become the same; see (e). 2 nC and long bunch case shows that the energy spread from 5 cm is always larger than 2 cm case; see (h). These results clearly show that we need careful consideration on the usage of the shielding since the evolution of the current profile along the dogleg is another significant factor in the real beamline.

Figure 4 shows the transverse and longitudinal beam parameter evolution for the EEX beamline (TDC on). While CSR affects on the transverse phase space via dispersion in the doglegs, it directly and indirectly changes

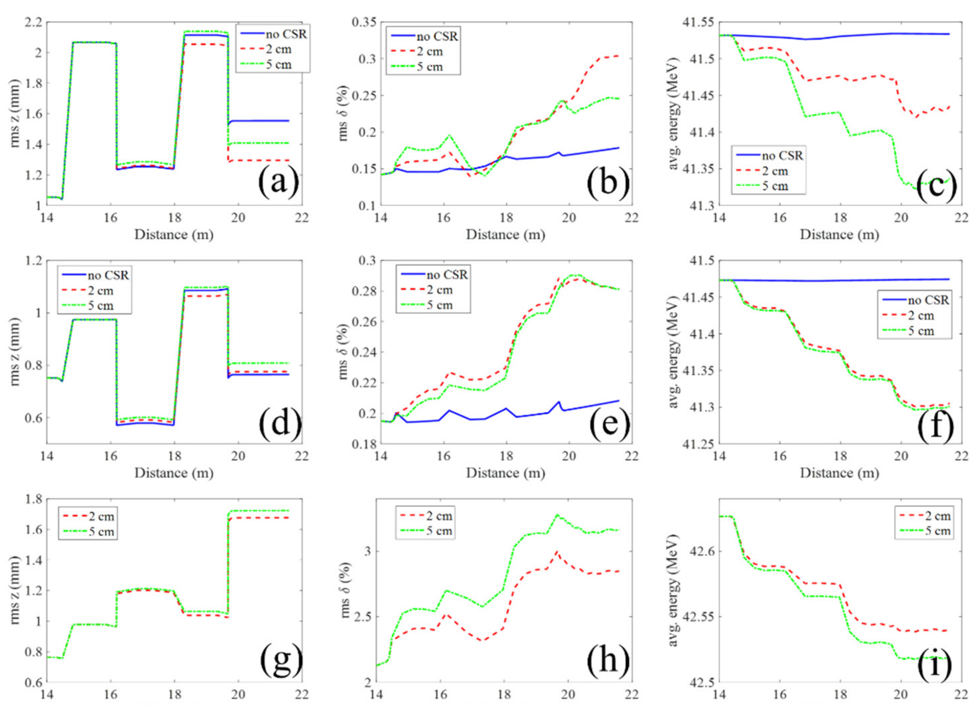

Figure 3: Evolution of longitudinal beam parameters along two doglegs. Each row corresponds to 10 nC beam, 2 nC beam with linac phase of -15°, and 2 nC beam with linac phase of -5°.

ISBN: 978-3-95450-184-7 doi:10.18429/JACoW-IPAC2018-TUPMK005

both transverse and longitudinal phase spaces in the EEX beamline due to phase space exchange process.

Longitudinal beam parameters follows normal tendency in this specific case (10 nC and long bunch); shorter bunch length, lower energy spread and lower emittance for the smaller gap. However, the transverse parameters show different result. While 5 cm gap generates a larger beam size and divergence, it generates a smaller transverse emittance. This tendency is originated from the beamline characteristics. In the dogleg, CSR changes the energy profile directly and the transverse profile via the dispersion. How the current profile evolves is the major consideration in the dogleg. However, the CSR effect in the EEX beamline is strongly entangled with the beamline characteristics since EEX beamline generates mix of the phase spaces. Thus, it is important to match the incident beam condition and the beamline to control the CSR and CSR shielding effect.

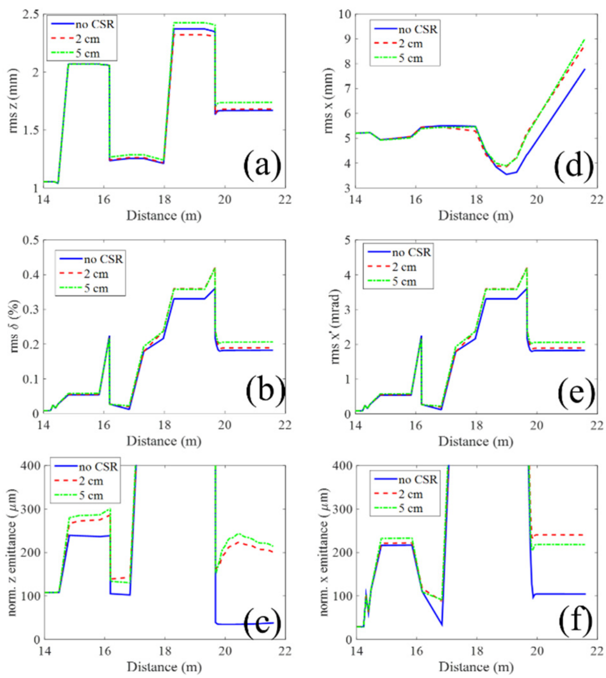

Figure 4: Evolution of beam parameters along a single EEX beamline. Each column shows longitudinal and transverse beam parameters. 10 nC beam is used for the simulation.

ACKNOWLEDGEMENT

This work is supported by Department of Energy, Office of Science, under contract No. DE-AC02-06CH11357.

REFERENCES

[1] R. Kato *et al.*, "Suppression of Coherent Synchrotron Radiation in Conducting Boundaries", in *Proc. PAC'93*, Washington, D.C., USA, May 1993, p. 1617-1619.

[2] R. Hajima *et al., Nucl. Instrum. Methods Phys. Res. Sec. A,* vol. 528, p. 335, 2004.

[3] C. Mitchell *et al.*, *Phys. Rev. Accel. Beams,* vol. 16, p. 060703, 2013.

[4] S. Di Mitri *et al.*, *Phys. Rev. Lett.,* vol. 110, p. 14801, 2013.

[5] M. W. Guetg *et al.*, *Phys. Rev. Accel. Beams,* vol. 18, p. 030701, 2015.

[6] R. Kato *et al.*, *Phys. Rev. E,* vol. 57, p. 3454, 1998.

[7] D. Sagan *et al.*, *Phys. Rev. ST Accel. Beams,* vol. 12, p. 040703, 2009.

[8] V. Yakimenko *et al.*, *Phys. Rev. Lett.,* vol. 109, p. 164802, 2012.

[9] G. Ha *et al.*, *Phys. Rev. Lett.,* vol. 118, p. 104801, 2017.

[10] www.pulsar.nl/gpt

[11] I. Bazarov and T. Miyajima, "Calculation of Coherent Synchrotron Radiation in General Particle Tracer", in *Proc. EPAC'08*, Genoa, Italy, June 2008, paper MOPC024, p. 118-120.